Dynamic Task Performance, Cohesion, and Communications in Human Groups

Luis Felipe Giraldo and Kevin M. Passino, *Fellow, IEEE*

Abstract—In the study of the behavior of human groups, it has been observed that there is a strong interaction between the cohesiveness of the group, its performance when the group has to solve a task, and the patterns of communication between the members of the group. Developing mathematical and computational tools for the analysis and design of task-solving groups that are not only cohesive but also perform well is of importance in social sciences, organizational management, and engineering. In this paper, we model a human group as a dynamical system whose behavior is driven by a task optimization process and the interaction between subsystems that represent the members of the group interconnected according to a given communication network. These interactions are described as attractions and repulsions among members. We show that the dynamics characterized by the proposed mathematical model are qualitatively consistent with those observed in real-human groups, where the key aspect is that the attraction patterns in the group and the commitment to solve the task are not static but change over time. Through a theoretical analysis of the system we provide conditions on the parameters that allow the group to have cohesive behaviors, and Monte Carlo simulations are used to study group dynamics for different sets of parameters, communication topologies, and tasks to solve.

Index Terms—Cohesion, consensus, human group dynamics, networks, task performance, ultimate boundedness.

I. INTRODUCTION

IN DISCIPLINES ranging from psychology, sociology, social work, and engineering, significant efforts have been undertaken to understand the dynamics of human groups, that is, the processes within the group resulting from the actions of its members and the interaction among each other and their environment [1]–[3]. Studies suggest that human groups cannot be examined by considering each member in isolation [4]. Elements, such as the situation the group is in, the particular characteristics of each individual, and his or her interactions with other group members, have to be considered for the analysis and understanding of the dynamics of the group. Lewin [5] provided a theoretical analysis of group dynamics where he states that a group is a dynamical system in which the behavior of a member is guided by the interplay between its individual features and the environment. "Environment" in this context includes other members of the group and the social setting. Lewin summarizes this process using the formula

$$B = \mathcal{I}(P, H) \qquad (1)$$

which describes a group member's dynamics (B) as a function ($\mathcal{I}$) of the interaction between his or her individual attributes (P) and the social environment (H). In this paper, we propose a mathematical characterization of group dynamics that is conceptually consistent with Lewin's formula. To model the function $\mathcal{I}$ of the interaction between a group member and the social environment he or she is in, we focus on the relationship between three important processes that affect the dynamics of a group: 1) cohesion between the group members; 2) performance of the group while solving a complex task; and 3) the patterns in the flow of information between members.

One of the most well studied concepts in the analysis of group dynamics is group cohesion. Cohesion is defined by Festinger [6] as "the resultant of all the forces acting on the members to remain in the group." According to Festinger, these forces depend on the attractiveness of each member to other members and to the activities that the group is participating in. Group cohesion then directly depends on the attractions between members, and has an important effect on group uniformity: a highly cohesive group is subject to pressures that result in uniformity among its members, that is, a consensus between the members of the group toward some goal [6]–[8]. Another important concept in the analysis of human group dynamics is group performance. Individuals work together in a way that their collective effort leads the group to have a good performance. Hence, the success of a task-oriented group is defined by its performance on a task [9]. Evidence suggests that there is a strong relationship between group cohesion and task-performance. Mullen and Copper [10] and Beal *et al.* [11] studied the results of different experiments that examined the relation between cohesion and performance in groups, and concluded that there is a bidirectional effect between group cohesion and task-performance: "cohesion makes groups more successful, but groups that succeed also become more cohesive" [3]. Cohesive groups are successful largely because the contributions of each group member are coordinated with those of the other members. At the same time, the success in groups tends to enhance the cohesiveness between the members of the group [3]. These studies suggest that in the bidirectional relation between performance and cohesion, the impact of performance on cohesion is stronger

than the impact of cohesion on performance [10]. The third concept in group dynamics that we consider in this paper is the structure of flow of information between members and its impact on performance and cohesion. In a group, members exchange information with other members of the group following a communication network. The study of the impact of the communication network topology (i.e., the pattern of interconnections) on the group has focused on the analysis of the effect of the degree of centralization and the number of group members on the performance and cohesion of the group. A group with a high degree of centrality is one in which an individual or few individuals serve as a hub for communications. Studies suggest that groups with communication networks that have a decentralized topology have a better performance than the centralized ones when the group has to solve complex tasks [12]–[14]. In these studies, tasks considered as complex had a higher number of task goals, pathways to complete the goals, and load of information than the ones considered as simple [15], [16]. Also, studies have shown that the number of people that interact with an individual affects both cohesion and performance. Too large of a number of individuals interacting with an individual results in a reduction of the performance and cohesion in the group [10].

Here, we propose a mathematical characterization of the dynamic behavior of human groups that is consistent with what has been observed in behavioral studies on cohesion, performance, and communication networks. The development of mathematical models of groups has gained a lot of attention from different disciplines. In social psychology, mathematical descriptions of the behavior of human groups have been studied. For example, Helbing [17] proposed a gradient-based model of the dynamics of individuals in a group. They introduce the concept of social force, which is a vector quantity that drives the behavior of an individual, and it depends on the interaction with other members of the group and external social influences such as trends, public opinions, and social norms. Pentland and Liu [18] studied the modeling and automatic recognition of human behavior under specific situations using statistical tools. The main assumption in the model is that the patterns in behavior of the individuals in a group can be described as the concatenation of multiple prototypical behaviors. Moussaïd *et al.* [19] modeled the behavior of pedestrians that walk in groups. Here, the motion of the pedestrians is directed by the action of a force that results from the combination of different components: the pedestrian's motivation to move in a desired direction, the repulsion effect to avoid collisions with other pedestrians and obstacles, and the social interaction with other members of the group. In engineering, there is a well-developed theoretical framework for the modeling and analysis of systems with multiple interactive agents [20]–[24]. It focuses on the modeling of systems that are composed of agents that have a behavior that depends on the interaction between them and follow a communication network that can be constant or changing in time. In that analysis, the main goal is to find the conditions that make the agents reach an agreement in different scenarios such as changes in the communication topology.

These models have been used in a variety of applications that include control of cooperative autonomous vehicles [25], distributed learning of pattern recognition models [26], and synchronization of microgrids in power systems [27].

Most of these models focus on describing the cohesive behavior of the groups, modeling the attraction forces acting on the individuals, and determining the conditions on the communication network and parameters of the model so that the group achieves certain stability properties. To our knowledge, modeling the relationship between cohesion and performance as observed in human groups has been overlooked. Our aim is to model the dynamics of a group that, given a network of communication between its members, not only tends to be cohesive but at the same time attempts to solve a complex task. Our contribution is twofold. First, we propose a computational model of the dynamics of human groups that have a communication network and work to solve a task, providing a mathematical formulation of Lewin's formula [5] that is consistent with the observations in real-human groups during task-solving processes. We do not try to propose models to recreate the specific experiments with humans that have been done to study these dynamics. Our aim is to design a mathematical model that characterizes dynamics that are qualitatively consistent with those observations in human groups. This paper is conceptually related to [17] and [28, Ch. 11], where the behavior of a group is modeled as the result of social forces acting on its members. The main difference is that this paper is focused on the development and analysis of a model that captures the relationship between cohesion and performance on the group given the patterns of information flow among its members. Second, we build on and extend the models of multiagent system dynamics in [20], [22], [23], and [29]. Gazi and Passino [20] and Liu and Passino [29] modeled the attraction and repulsion dynamics of groups of individuals that are evaluated according to a performance function or "resource environment," and Li [22] and Yu *et al.* [23] extended these results to the case where there is a weighted communication topology that defines the patterns in communication between the individuals. In this paper, we formulate a model of a group of individuals that interact according to a general communication network topology, where the attraction weights and the commitment to optimize the performance function change over time (Section II). We show that a key aspect for a cohesive group to be successful (i.e., having a good performance) is that the attraction patterns between the members of the group and the commitment to solve the task are not static but dynamic and develop over time, playing an important role in shaping the behavior of the group. We provide a mathematical analysis of group cohesiveness that is an extension of the analysis developed in [29, Th. 1], where we study the conditions in our model that allow the group to be cohesive (Section III). Moreover, we show through simulations (Section IV) the impact of the parameters of the model and the communication networks on the behavior of the group in terms of group performance and group cohesion when the group is required to solve a complex task.

II. MATHEMATICAL MODEL

We propose a mathematical formalization of Lewin's formula (1) that characterizes the dynamics of the behavior of each group member. We model the group as a network of interconnected dynamical systems in which a group member's variables are driven by his/her personal characteristics, interaction with the other members, and performance in solving a given task. One of the main features of our model is that the interaction patterns of an individual and his/her commitment to solve a task are not static, but develop over time.

A. Model Formulation

The network that describes how the group members are interconnected is represented by a directed graph $\mathcal{G} = (\mathcal{V}, \mathcal{E})$, where $\mathcal{V} = \{1, 2, \ldots, N\}$ denotes the set of labels of the N individuals of the group, and $\mathcal{E} \subseteq \mathcal{V} \times \mathcal{V}$ is the set of edges of the graph. Edge (i, j) in $\mathcal{E}$ indicates that individual i gets information from individual j. All group members that supply information to individual i are $\mathcal{N}_i = \{j : (i, j) \in \mathcal{E}\}$. Hence, $\mathcal{G}$ defines the communication patterns between the members of the group. Let $x^i \in \mathbb{R}^p$ be a vector of measurable variables that indicate the "state" of the individual in the task-solving process. In models of human decision processes, these variables typically include preferences of the individual, and attributes of the alternatives that are involved in the task [30], [31]. We refer to $x^i(t)$ as the position of individual i at given time t, and motion refers to a change in position with respect to time. "Position" here is not necessarily physical location, but can represent "viewpoint" or "opinion."

Let $f : \mathbb{R}^p \to \mathbb{R}$ be a continuously differentiable function that evaluates the position of an individual according to the task assigned to the group and quantifies its performance. We assume that lower values of f correspond to better positions. The behavior of an individual in the group is assumed to be directly influenced by his or her characteristics, performance during the task-solving process, and interaction with other members of the group. We refer to these influences as forces that determine the individual's behavior. "Force" is not necessarily the one from physics with units of Newton, but simply represents "influence" of some sort. To provide a mathematical formalization of Lewin's formula for behavior, we characterize the interaction function $\mathcal{I}$ in (1) from the perspective of Newton's second law: forces acting on the group and driving its behavior. We assume that the behavior of individual i can be described by

$$\dot{x}^i(t) = v^i(t)$$
$$\dot{v}^i(t) = \frac{1}{M^i} u^i(t) \tag{2}$$

where $t \in \mathbb{R}_{\geq 0}$ is the time variable, $\dot{x}^i(t)$ denotes the derivative of x^i with respect to t, and $v^i(t)$ is its velocity at time t. The acceleration of the individual is $\dot{v}^i(t)$, and $u^i(t)$ is the force vector that drives the motion of the individual. The variable M^i then corresponds to the mass of individual i if it has mass, or more generally, it is a parameter that affects the influence of u^i on the dynamics of group member i. It represents a parameter that affects the tendency of viewpoint or opinion to change.

The force u^i is defined by four different components

$$u^i(t) = p^i(t) + a^i(t) + r^i(t) - \zeta_i v^i(t) \tag{3}$$

where $p^i(t)$ is the force component that provides the direction that optimizes the performance of individual i at time t. Since lower values of $f(x^i(t))$ indicate a better performance of i, we define $p^i(t)$ such that it points toward positions where f is reduced. Hence, we choose $p(t)$ to move along the (scaled) negative gradient of f evaluated at $x^i(t)$

$$p^i(t) = -\eta^i(t)\nabla f(x^i(t)) \tag{4}$$

where $\nabla f(x^i(t))$ is the gradient of f evaluated at $x^i(t)$, and $\eta^i(t)$ is the magnitude of the influence of the performance on the individual's motion. Later, we will define the dynamics of $\eta^i(t)$ and show that $\eta^i(t) \geq 0$ for all $t \geq 0$ if $\eta^i(0) \geq 0$, $i = 1, \ldots, N$.

The second component of u^i in (3) is the attraction of i to every $j \in \mathcal{N}_i$ in position and velocity, and it is defined as

$$a^i(t) = -\frac{1}{|\mathcal{N}_i|} \sum_{j \in \mathcal{N}_i} \left[w^{ij}(t)(x^i(t) - x^j(t)) \right. $$
$$\left. + bw^{ij}(t)(v^i(t) - v^j(t)) \right] \tag{5}$$

where $|\mathcal{N}_i|$ is the number of individuals that communicate with i, and $w^{ij}(t) \geq 0$, $t \geq 0$ is the attraction strength of individual i to individual $j \in \mathcal{N}_i$, with $b \geq 0$. We have that $-w^{ij}(t)(x^i(t) - x^j(t))$ is the component of $a^i(t)$ associated with the attraction in position of i to some $j \in \mathcal{N}_i$. It indicates that a larger separation between individuals implies a larger attraction of i in the direction of j. A similar statement can be made for the attraction in velocity. Note that the attraction strengths w^{ij} can be represented as weights associated to the edges of the graph $\mathcal{G}$.

The next force component in (3) is the short-range repulsion between the group members. We allow the model to include behaviors where a group member tries to avoid having the same position as the other members he or she communicates with to allow some degree of variability during the process of solving the task. Let $r^i(t)$ be the repulsion of i from the individuals in $\mathcal{N}_i$ on short distances given by

$$r^i(t) = \frac{1}{|\mathcal{N}_i|} \sum_{j \in \mathcal{N}_i} \kappa^{ij}$$
$$\exp\left(-\frac{1}{2\beta_{ij}^2}\|x^i(t) - x^j(t)\|^2\right)(x^i(t) - x^j(t)) \tag{6}$$

where $\kappa^{ij} \geq 0$ and $\beta^{ij} \geq 0$. Term $\kappa^{ij}\exp(-(1/2\beta_{ij}^2)\|x^i(t) - x^j(t)\|^2)(x^i(t) - x^j(t))$ corresponds to the component of the force that makes individual i be repelled by individual j, where κ^{ij} is the repulsion strength and $\exp(-(1/2\beta_{ij}^2)\|x^i(t) - x^j(t)\|^2)$ defines the radius of action of the repulsion. We also have the force component $-\zeta^i v^i(t)$, $\zeta^i > 0$, which points toward the opposite direction of the velocity vector v^i. This term produces a reduction in the velocity of the individual.

A key aspect in human group processes is that the attraction patterns among the group members and their commitment to solving a task are not static but dynamic and develop over time [3]. In our model, we characterize the dynamics of the attraction and performance strengths defined in (4) and (5) based on the observations that: 1) individuals tend to be more attracted to those group members that are performing better during the task-solving process [3] and 2) group dynamics tend to reach a consensus among members to move toward some goal [6]. We first describe the dynamics of the attraction strengths using a growth model that makes the individuals be more attracted to those that have better relative performance in solving the given task as follows:

$$\dot{w}^{ij}(t) = \alpha_w \left(w^{ij}(t) - C_w^l \right)\left(C_w^u - w^{ij}(t) \right)\Delta f^{ij}(t) \quad (7)$$

where $\alpha_w > 0$ is the growth rate, and $\Delta f^{ij}(t) = (f(x^i(t)) - f(x^j(t)))/\sum_{k \in \mathcal{N}_i} f(x^k(t))$ is the scaled difference between the performance function of individuals i and j. The strength of attraction of i toward j increases when $f(x^i) > f(x^j)$, i.e., when individual j is performing better than i, and decreases when $f(x^i) < f(x^j)$. Recall that lower values of f correspond to better performance of the individual. Note that C_w^l and C_w^u are equilibrium points of the system (7), where $0 \geq C_w^l \geq C_w^u$, and $\dot{w}^{ij}(t) > 0$ when $\Delta f^{ij}(t) > 0$ and $\dot{w}^{ij}(t) < 0$ when $\Delta f^{ij}(t) < 0$, for all $w^{ij}(t) \in (C_w^l, C_w^u)$. This means that the trajectories of w^{ij} are bounded below by C_w^l and above by C_w^u for all $t \geq 0$ if $w^{ij}(0) \in [C_w^l, C_w^u]$, and their rate of change and direction are affected by $\alpha_w \Delta f^{ij}(t)$. The strength of the force component associated with performance optimization has dynamics given by the growth model

$$\dot{\eta}^i(t) = \alpha_\eta \eta^i(t)(C_\eta - \eta^i(t))$$
$$\left(B_\eta - \frac{1}{|\mathcal{N}_i|} \sum_{j \in \mathcal{N}_i} \left\| x^j(t) - x^i(t) \right\|^2 \right) \quad (8)$$

where $\alpha_\eta > 0$ is the growth rate, and $B_\eta > 0$ is a threshold parameter that determines the sign of the growth rate. The strength of the performance optimization component of the motion's force of individual i decreases when $|\mathcal{N}_i|^{-1} \sum_{j \in \mathcal{N}_i} \| x^j - x^i \|^2$ is larger than B_η, that is, when the group is not cohesive. This dynamical model allows force u^i in (3) to be more influenced by the attraction between the members of the group than the commitment to solve the task when the group is not cohesive enough. The trajectories of η^i are bounded below by zero and above by C_η when $\eta^i(0) \geq 0$.

In Section IV, we show that (7) and (8) play a fundamental role in modeling dynamics that are consistent with the observations in human groups during a task-solving process in terms of cohesion and performance.

B. Optimization Point of View for the Model

We can analyze the role of each one of the components of the driving force u^i from an optimization point of view. The dynamics characterized by the model in (2) and (3) can be viewed as the result of minimizing a set of cost functions that are involved in the task-solving process by the group. Let $L_a^j(x^i(t), v^i(t)) \in \mathbb{R}$ be a function of $x^i(t)$ and $v^i(t)$ that

measures how far individual i is to individual $j \in \mathcal{N}_i$ in position and velocity defined as

$$L_a^j\left(x^i(t), v^i(t)\right) = \frac{1}{2} w^{ij}(t)\left\| x^i(t) - x^j(t) \right\|^2$$
$$+ \frac{1}{2} b w^{ij}(t)\left\| v^i(t) - v^j(t) \right\|^2. \quad (9)$$

This function can be seen as a weighted squared error between the velocity and position of j with respect to a given i. Let $L_r^j(x^i(t)) \in \mathbb{R}$ be a function of $x^i(t)$ defined as

$$L_r^j\left(x^i(t)\right) = \frac{1}{2} \hat{\kappa}^{ij} \exp\left(-\frac{1}{2\beta_{ij}^2} \left\| x^i(t) - x^j(t) \right\|^2 \right). \quad (10)$$

This is a Gaussian function of $x^i(t)$ centered at $x^j(t)$, with amplitude and width controlled by $\hat{\kappa}^{ij} \geq 0$ and β_{ij}. It has its highest value at $x^i(t) = x^j(t)$, and decreases as $x^i(t)$ moves away from $x^j(t)$. Let

$$q_v\left(v^i(t)\right) = \frac{1}{2} \left\| v^i(t) \right\|^2 \quad (11)$$

be a function of $v^i(t)$ with a unique minimum at $v^i(t) = 0$. Using (9)–(11) we define the cost function

$$L\left(x^i(t), v^i(t)\right) = \eta^i f\left(x^i(t)\right) + \frac{1}{|\mathcal{N}_i|} \sum_{j \in \mathcal{N}_i} L_a^j\left(x^i(t), v^i(t)\right)$$
$$+ \frac{1}{|\mathcal{N}_i|} \sum_{j \in \mathcal{N}_i} L_r^j\left(x^i(t)\right) + \zeta_i q_v\left(v^i(t)\right). \quad (12)$$

Let ∇_x and ∇_v denote the gradient operator with respect to the position and velocity vectors. The gradient of L with respect to $x^i(t)$ and $v^i(t)$ is given by

$$\nabla_x L\left(x^i(t)\right) = \eta^i(t)\nabla_x f(x(t)) + \frac{1}{|\mathcal{N}_i|} \sum_{j \in \mathcal{N}_i} \nabla_x L_a^j\left(x^i(t)\right)$$
$$+ \frac{1}{|\mathcal{N}_i|} \sum_{j \in \mathcal{N}_i} \nabla_x L_r^j\left(x^i(t)\right) \quad (13)$$

$$\nabla_v L\left(v^i(t)\right) = \frac{1}{|\mathcal{N}_i|} \sum_{j \in \mathcal{N}_i} \nabla_v L_a^j\left(v^i(t)\right) + \zeta_i \nabla_v q_v\left(v^i(t)\right). \quad (14)$$

Using (13) and (14), we can rewrite force $u^i(t)$ in (3) as

$$u^i(t) = -\nabla_x L\left(x^i(t)\right) - \nabla_v L\left(v^i(t)\right). \quad (15)$$

This expression shows us that the force $u^i(t)$ points to the opposite direction of the gradient of the cost function L, that is, the motion of individual i tends to minimize L with respect to the position and velocity. According to this, we have that the attraction term in (5) can be rewritten as

$$a^i(t) = -\frac{1}{|\mathcal{N}_i|} \sum_{j \in \mathcal{N}_i} \left[\nabla_x L_a^j\left(x^i(t)\right) + \nabla_v L_a^j\left(v^i(t)\right) \right]$$

which is the vector that points to the direction that minimizes the error in position and velocity between i and j. Also, the repulsion term in (6) can be rewritten as the vector that points to the direction that minimizes the Gaussian function L_r^j, for every $j \in \mathcal{N}_i$ as follows:

$$r^i(t) = -\frac{1}{|\mathcal{N}_i|} \sum_{j \in \mathcal{N}_i} \nabla_x L_r^j\left(x^i(t)\right).$$

The velocity damping term in $u^i(t)$ corresponds to the vector $-\zeta_i \nabla_v q_v(v^i(t))$, which points to the direction in which the velocity is minimized.

Equation (15) shows that the dynamics of each member of the group can be seen as the result of a continual optimization process with respect to his or her position and velocity, where the objective function changes over time and is interconnected with those of the other members of the group. Note that depending on the selection of the parameters of the cost function L, the descent direction will be biased toward the minimization of those components with higher magnitude. In Section IV, we will show that the cost function changes over time such that there is an interaction between the performance optimization component f and attraction component L_a^j that allows the minimization process to achieve a solution that involves a tradeoff between them.

III. CONDITIONS FOR COHESIVE BEHAVIOR OF THE GROUP

In a cohesive group, each individual behaves in a way that its position and velocity during the task-solving process ultimately are close to those of the other members of the group. Here, we analyze the conditions that allow the group to exhibit cohesive behaviors while solving a task and under an assumed communication network topology. Without loss of generality, we assume that $M^i = 1$, $\zeta^i = \zeta$, $\zeta > 0$, for $i = 1, \ldots, N$. Also, to facilitate the notation in this analysis, we do $\tilde{w}^{ij}(t) = w^{ij}(t)/|\mathcal{N}_i|$ for every $i = 1, \ldots, N$ and $j \in \mathcal{N}_i$. We define the error in position and velocity between individuals i and j

$$e_x^{ij} = x^i - x^j$$
$$e_v^{ij} = v^i - v^j.$$

In a cohesive group, the error in position and velocity reaches a point where every two members of the group are considered close to each other. To analyze the cohesion of the group we study the dynamics of the error in position and velocity of the individuals in the group. The error dynamics are given by

$$\dot{e}_x^{ij} = \dot{x}^i - \dot{x}^j = e_v^{ij}$$
$$\dot{e}_v^{ij} = \dot{v}^i - \dot{v}^j$$
$$= -\sum_{k \in \mathcal{N}_i} \tilde{w}^{ik}(t) e_x^{ik} - \sum_{k \in \mathcal{N}_i} \left(b\tilde{w}^{ik}(t) + \zeta\right) e_v^{ik} + g^{ij} + \delta^{ij} + \phi^{ij}$$

where

$$\phi^{ij} = \sum_{l \in \mathcal{N}_j} \tilde{w}^{jl}(t)\left(e_x^{jl} + be_v^{jl}\right) \tag{16}$$

$$g^{ij} = -\eta^i(t)\nabla f\left(x^i(t)\right) + \eta^j(t)\nabla f\left(x^j(t)\right) \tag{17}$$

$$\delta^{ij} = \frac{1}{|\mathcal{N}_i|}\sum_{k \in \mathcal{N}_i} \kappa^{ik}$$
$$\exp\left(-\frac{1}{2\beta_{ik}^2}\left\|x^i(t) - x^k(t)\right\|^2\right)\left(x^i(t) - x^k(t)\right)$$
$$- \frac{1}{|\mathcal{N}_j|}\sum_{l \in \mathcal{N}_j} \kappa^{jl}$$
$$\exp\left(-\frac{1}{2\beta_{jl}^2}\left\|x^j(t) - x^l(t)\right\|^2\right)\left(x^j(t) - x^l(t)\right). \tag{18}$$

Let $E^{ij} = [e_x^{ij\top}, e_v^{ij\top}]^\top$. The system can be written in matrix form as

$$\dot{E}^{ij} = \sum_{j \in \mathcal{N}_i} \overbrace{\begin{bmatrix} 0_p & I_p \\ -\tilde{w}^{ij}(t)I_p & -(b\tilde{w}^{ij}(t) + \zeta)I_p \end{bmatrix}}^{A_{ij}(t)} E^{ij}$$
$$+ \overbrace{\begin{bmatrix} 0_p \\ I_p \end{bmatrix}}^{B}(g^{ij} + \delta^{ij} + \phi^{ij}) \tag{19}$$

where I_p and 0_p are the $p \times p$ identity and zero matrices. Note that $A_{ij}(t)$ in (19) is a time-varying matrix that has eigenvalues given by the roots of the polynomial $(\lambda^2 + (b\tilde{w}^{ij}(t) + \zeta)\lambda + \tilde{w}^{ij}(t))^p$. Since we assume that $\tilde{w}^{ij}(t) > 0$ for all $t \geq 0$, then the eigenvalues of $A_{ij}(t)$ have negative real part for all $t \geq 0$. The following theorem specifies conditions that are sufficient for the group to reach a state in which the group is considered cohesive.

Theorem 1: Consider the group whose dynamics are characterized by the model in (2)–(8). Assume that $C_w^l < w^{ij}(0) < C_w^u$, for all $i = 1, \ldots, N$, $j \in \mathcal{N}_i$. Also, assume that the difference in performance between two members of the group in (7) and the component of the force u_i in (3) that seeks to optimize the performance of the individuals in the group are bounded during the task-solving process, i.e., there exist constants $\psi \geq 0$ and $\psi_g \geq 0$ such that

$$\left|\Delta f^{ij}(t)\right| \leq \psi, \quad \forall t \geq 0 \tag{20}$$
$$\|\nabla f(x)\| \leq \psi_g \tag{21}$$

for all $x \in \mathbb{R}^p$, $i = 1, \ldots, N$, and $j \in \mathcal{N}_i$. Let the parameters of the model be such that, for all $t \geq 0$

$$c_1^{ij} > 0 \tag{22}$$

and

$$\frac{c_3^{ij}|\mathcal{N}_j| + \sum_{l \in \Gamma_i} c_3^{li}}{2(1 - \theta_{ij})} < c_1^{ij} \tag{23}$$

for some $\theta^{ij} \in (0, 1)$, $i = 1, \ldots, N$, $j \in \mathcal{N}_i$, where Γ_i is the set of members of the group that has i as a neighbor in the communication network, and

$$c_1^{ij} = \max_{\tilde{w}^{ij} \in \left[\frac{C_w^l}{|\mathcal{N}_i|}, \frac{C_w^u}{|\mathcal{N}_i|}\right]} 2\tilde{w}^{ij} - \left[b + \frac{\zeta(1 + 2\tilde{w}^{ij}) + b(\tilde{w}^{ij})^2}{(\zeta + b\tilde{w}^{ij})^2}\right] \alpha_w(|\mathcal{N}_i|\tilde{w}^{ij} - C_w^l)(C_w^u - |\mathcal{N}_i|\tilde{w}^{ij})\psi \tag{24}$$

$$c_3^{ij} = \max_{\tilde{w}^{ij} \in \left[\frac{C_w^l}{|\mathcal{N}_i|}, \frac{C_w^u}{|\mathcal{N}_i|}\right]} \left[\frac{(\zeta + b\tilde{w}^{ij})^2 + (\tilde{w}^{ij} + 1)^2}{\zeta + b\tilde{w}^{ij}} + \sqrt{2(\tilde{w}^{ij})^2 + (\zeta + b\tilde{w}^{ij})^2 + \frac{((\tilde{w}^{ij})^2 - 1)^2}{(\zeta + b\tilde{w}^{ij})^2}}\right]$$
$$\times \sqrt{1 + b}. \tag{25}$$

Then, the trajectories of the error system in (19) for every $i = 1, \ldots, N$ and $j \in \mathcal{N}_i$ are uniformly ultimately bounded.

Furthermore, if the topology of the communication network in the group is strongly connected, i.e., there is a directed path

between every two nodes, then the trajectories of the error between every pair of individuals in the group are uniformly ultimately bounded.

Proof: The Lyapunov function chosen to do the cohesiveness analysis of the system in (19) is

$$V(t, E) = \sum_{i=1}^{N} \sum_{j \in \mathcal{N}_i} V^{ij}(t, E) \tag{26}$$

where E is the vector containing all the errors E^{ij}. The functions $V^{ij}(E)$ are given by

$$V^{ij}(t, E) = E^{ij\top} P_{ij}(t) E^{ij}$$

where $P_{ij}(t)$ is a $2p \times 2p$ time-varying matrix such that $P_{ij}(t) = P_{ij}(t)^\top > 0$ for all $t \geq 0$. The derivative of $V^{ij}(t, E)$ along the trajectories of the system in (19) is given by

$$
\begin{aligned}
\dot{V}^{ij}(t, E) = {}& E^{ij\top} \dot{P}_{ij}(t) E^{ij} \\
&+ E^{ij\top} \left(A_{ij}^\top P_{ij}(t) + P_{ij}(t) A_{ij} \right) E^{ij} \\
&+ \left[B\left(g^{ij} + \delta^{ij} + \phi^{ij} \right) \right]^\top P_{ij}(t) E^{ij} \\
&+ E^{ij\top} P_{ij}(t) B\left(g^{ij} + \delta^{ij} + \phi^{ij} \right).
\end{aligned} \tag{27}
$$

From [32, Th. 4.6] and [33], given a matrix $Q_{ij}(t) > 0$ and a matrix $A_{ij}(t)$ that has all its eigenvalues with negative real part for all $t \geq 0$, we can find $P_{ij}(t)$ such that $-Q_{ij}(t) = P_{ij}(t)A_{ij}(t) + A_{ij}(t)^\top P_{ij}(t)$, for all $t \geq 0$. Using this result, we can rewrite (27) as

$$
\begin{aligned}
\dot{V}^{ij}(t, E) = {}& E^{ij\top} \left[\dot{P}_{ij}(t) - Q_{ij}(t) \right] E^{ij} \\
&+ \left[B\left(g^{ij} + \delta^{ij} + \phi^{ij} \right) \right]^\top P_{ij}(t) E^{ij} \\
&+ E^{ij\top} P_{ij}(t) B\left(g^{ij} + \delta^{ij} + \phi^{ij} \right).
\end{aligned} \tag{28}
$$

If we choose $Q_{ij}(t) = 2\tilde{w}^{ij}(t) I_{2p}$, the matrix $P_{ij}(t)$ that satisfies the above relation is

$$
P_{ij}(t) = \begin{bmatrix} \frac{\left(b\tilde{w}^{ij}(t)+\zeta\right)^2 + \tilde{w}^{ij}(t)\left(1+\tilde{w}^{ij}(t)\right)}{b\tilde{w}^{ij}(t)+\zeta} I_p & I_p \\ I_p & \frac{\left(1+\tilde{w}^{ij}(t)\right)}{b\tilde{w}^{ij}(t)+\zeta} I_p \end{bmatrix}.
$$

Its maximum eigenvalue satisfies $\lambda_{\max}\left[P_{ij}(t)\right] \leq c_3^{ij}|\mathcal{N}_i|/(2C_w^u\sqrt{1+b^2})$ for all $t \geq 0$, where c_3^{ij} is defined in (25). Matrix $P_{ij}(t)$ is a time-varying matrix whose entries depend on $\tilde{w}^{ij}(t)$, where its derivative with respect to t is

$$
\begin{aligned}
\dot{P}_{ij} &= \dot{\tilde{w}}^{ij} \frac{\partial P_{ij}}{\partial \tilde{w}^{ij}} \\
&= \dot{\tilde{w}}^{ij} \begin{bmatrix} \left[b + \frac{\zeta\left(1+2\tilde{w}^{ij}(t)\right)+b\tilde{w}^{ij}(t)^2}{\left(\zeta+b\tilde{w}^{ij}(t)\right)^2} \right] I_p & 0_p \\ 0_p & \frac{\zeta-b}{\left(\zeta+b\tilde{w}^{ij}(t)\right)^2} I_p \end{bmatrix}
\end{aligned}
$$

where $\dot{\tilde{w}}^{ij}$ is defined in (7). The maximum eigenvalue of the matrix $\dot{P}_{ij}(t) - Q_{ij}(t)$ satisfies $\lambda_{\max}[\dot{P}_{ij}(t) - Q_{ij}(t)] \leq -c_1^{ij}$, for all $t \geq 0$, where c_1^{ij} is defined in (24). This information will be useful to obtain an upper bound for $\dot{V}^{ij}(t, E)$ in (28).

Now, we study the remaining elements in (28). It can be shown that $\exp(-1/2)\beta$ is the unique maximum value of the function $h(y) = \exp(-1/2\beta^2 \|y\|^2)y$, for all $y \in \mathbb{R}^p$. Using this in (18), we obtain

$$
\begin{aligned}
\|\delta^{ij}\| &\leq \exp(-1/2)\left(\frac{1}{|\mathcal{N}_i|}\sum_{k \in \mathcal{N}_i} \kappa^{ij}\beta_{ij} + \frac{1}{|\mathcal{N}_j|}\sum_{l \in \mathcal{N}_j} \kappa^{jl}\beta_{jl} \right) \\
&= \bar{\delta}^{ij}.
\end{aligned} \tag{29}
$$

From (16), we have

$$
\begin{aligned}
\|\phi^{ij}\| &\leq \sum_{l \in \mathcal{N}_j} \tilde{w}^{jl}(t)\sqrt{1+b^2} \left\| E^{jl} \right\|, \quad j \in \mathcal{N}_i \\
&\leq C_w^u \sqrt{1+b^2} \sum_{l \in \mathcal{N}_j} \left\| E^{jl} \right\|
\end{aligned} \tag{30}
$$

where we used the fact that $\tilde{w}^{jl} < C_w^u/|\mathcal{N}_j|$, and $|\mathcal{N}_j| \geq 1$. From the assumption in (21), and since we know from (8) that $\eta^i \geq C_\eta$, we obtain

$$\|g^{ij}\| \leq 2C_\eta \psi_g. \tag{31}$$

Assume that (22) is satisfied. Then, putting (29)–(31) together in (28), and since $\|P_{ij}B\| \leq \lambda_{\max}[P_{ij}] \leq c_3^{ij}|\mathcal{N}_i|/(2C_w^u\sqrt{1+b^2})$ and

$$
\begin{aligned}
E^{ij\top}\left[\dot{P}_{ij}(t) - Q_{ij}(t)\right]E^{ij} &\leq \lambda_{\max}\left[\dot{P}_{ij}(t) - Q_{ij}(t)\right]\left\|E^{ij}\right\|^2 \\
&\leq -c_1^{ij}\left\|E^{ij}\right\|^2
\end{aligned}
$$

we obtain

$$\dot{V}^{ij}(E) \leq -c_1^{ij}\left\|E^{ij}\right\|^2 + c_2^{ij}\left\|E^{ij}\right\| + c_3^{ij}\left\|E^{ij}\right\|\sum_{l \in \mathcal{N}_j}\left\|E^{jl}\right\| \tag{32}$$

where $c_2^{ij} = [c_3^{ij}|\mathcal{N}_i|/(C_w^u\sqrt{1+b^2})](\bar{\delta}^{ij} + 2C_\eta\psi_g)$. Note that, for any $0 < \theta^{ij} < 1$, (32) can be written as

$$
\begin{aligned}
-c_1^{ij}\left\|E^{ij}\right\|^2 + c_2^{ij}\left\|E^{ij}\right\| &\leq -(1-\theta^{ij})c_1^{ij}\left\|E^{ij}\right\|^2 \\
&\forall \left\|E^{ij}\right\| > r^{ij} = -\sigma^{ij}\left\|E^{ij}\right\|^2
\end{aligned} \tag{33}
$$

where $r^{ij} = c_2^{ij}/(c_1^{ij}\theta^{ij})$ and $\sigma^{ij} = (1-\theta^{ij})c_1^{ij} > 0$. This indicates that the first two terms of the right-hand side of (32) are negative when $\|E^{ij}\| > r^{ij}$.

To find the conditions that make $\dot{V} < 0$ in (26), we define the sets Π_O^i and Π_I^i

$$
\begin{aligned}
\Pi_O^i &= \left\{ j : \left\|E^{ij}\right\| \geq r^{ij}, j \in \mathcal{N}_i \right\} \\
\Pi_I^i &= \left\{ j : \left\|E^{ij}\right\| < r^{ij}, j \in \mathcal{N}_i \right\}.
\end{aligned}
$$

The sets Π_O^i and Π_I^i contain the indices of the neighbors of i whose error E^{ij} at a given time satisfy $\|E^{ij}\| \geq r^{ij}$ and $\|E^{ij}\| < r^{ij}$, respectively. The size of the sets is $N_O^i = |\Pi_O^i|$ and $N_I^i = |\Pi_I^i|$. We first analyze the case when $1 \leq N_O^i \leq |\mathcal{N}_i|$, and later we discuss the case when $N_O^i = 0$. In the first case, since $\mathcal{N}_i = \Pi_O^i \cup \Pi_I^i$, we can set bounds on the components in $\dot{V}_{ij}$ that

depend on the $\|E^{ij}\|$ with $j \in \Pi_I^i$. Hence, from (26), (32), and (33), we obtain

$$
\begin{aligned}
\dot{V}(E) &= \sum_{i=1}^{N} \sum_{j \in \mathcal{N}_i} \dot{V}^{ij}(E) \\
&\leq \left[\sum_{i=1}^{N} \sum_{j \in \Pi_O^i} \left(-\sigma^{ij} \|E^{ij}\|^2 \right. \right. \\
&\quad \left. \left. + c_3^{ij} \|E^{ij}\| \sum_{l \in \Pi_O^j} \|E^{jl}\| \right) \right] \\
&\quad + \left[\sum_{i=1}^{N} \left(\sum_{j \in \Pi_O^i} c_3^{ij} K_1^{ij} \|E^{ij}\| \right) \right. \\
&\quad \left. + \sum_{i=1}^{N} \left(K_3^i \sum_{k \in \mathcal{N}_i} \sum_{l \in \Pi_O^k} c_3^{ik} \|E^{kl}\| \right) \right] \\
&\quad + K_2.
\end{aligned}
\tag{34}
$$

Here, we use the fact that for the $\|E^{ij}\| < r^{ij}$ with $j \in \Pi_I^i$ and $i = 1, \ldots, N$, there exist positive constants K_1^{ij}, K_2, and K_3^i that satisfy [29, Th. 1]

$$
K_1^{ij} \geq \sum_{l \in \Pi_I^j} \|E^{jl}\|, \quad j \in \mathcal{N}_i
$$

$$
K_2 \geq \sum_{i=1}^{N} \sum_{j \in \Pi_I^i} \left[-c_1^{ij} \|E^{ij}\|^2 + c_2^{ij} \|E^{ij}\| \right. \\
\left. + c_3^{ij} \|E^{ij}\| \sum_{l \in \Pi_I^j} \|E^{jl}\| \right]
$$

$$
K_3^i \geq \sum_{j \in \Pi_I^i} \|E^{ij}\|.
$$

The first term in brackets on the right-hand side of (34) is a quadratic form of the variables $\|E^{ij}\|$, $i = 1, \ldots, N$, $j \in \Pi_O^i$. Let y be a column vector of dimension $\sum_{i=1}^{N} |\Pi_O^i|$ with entries given by all the $\|E^{ij}\|$ for $i = 1, \ldots, N$, $j \in \Pi_O^i$. The quadratic form can be written as $y^\top S y$, where S is a squared matrix whose diagonal elements are given by $-\sigma^{ij}$, and the off-diagonal elements depend on the variables c_3^{ij}. We know that $y^\top S y < 0$ if and only if the eigenvalues of its symmetric part $(S + S^\top)/2$ are negative. According to the Gershgorin circle theorem [34, Ch. 7], all its eigenvalues λ satisfy

$$
|\lambda + \sigma^{ij}| \leq \frac{1}{2} \left(c_3^{ij} |\Pi_O^j| + \sum_{l \in \Gamma_i} c_3^{li} \right)
\tag{35}
$$

where $\Gamma_i = \{j : j \in \{1, \ldots, N\}, i \in \mathcal{N}_j\}$, that is, Γ_i is the set of nodes that has node i as a neighbor. The right-hand side of (35) corresponds to the sum of the elements of the row of $(S + S^\top)/2$ associated with the variable $\|E^{ij}\|$, where $c_3^{ij} |\Pi_O^j|$ and $\sum_{l \in \Gamma_i} c_3^{li}$ are the sum of the elements of the ith

row of S and $S^\top$, respectively. Then, a sufficient condition for the quadratic form to be negative definite is

$$
-\sigma^{ij} + \frac{1}{2} \left(c_3^{ij} |\Pi_O^j| + \sum_{l \in \Gamma_i} c_3^{li} \right) < 0.
\tag{36}
$$

Note that this is satisfied if (22) and (23) are satisfied. Assume that these conditions are satisfied, and the first term in brackets on the right-hand side of (34) is negative. Then, $\lambda_{\max}[(S + S^\top)/2] < 0$, and

$$
\begin{aligned}
\dot{V}(E) &\leq \left[\lambda_{\max}\left[(S + S^\top)/2 \right] \sum_{i=1}^{N} \sum_{j \in \Pi_O^i} \|E^{ij}\|^2 \right] \\
&\quad + \left[\sum_{i=1}^{N} \sum_{j \in \Pi_O^i} c_3^{ij} K_1^{ij} \|E^{ij}\| \right. \\
&\quad \left. + \sum_{i=1}^{N} K_3^i \sum_{k \in \mathcal{N}_i} \sum_{l \in \Pi_O^k} c_3^{ik} \|E^{kl}\| \right] + K_2.
\end{aligned}
\tag{37}
$$

Then, from (37), when $\|E^{ij}\|$, $i = 1, \ldots, N$, $j \in \Pi_O^i$, is sufficiently large, the term

$$
\lambda_{\max}[(S + S^\top)/2] \sum_{i=1}^{N} \sum_{j \in \Pi_O^i} \|E^{ij}\|^2
$$

determines the sign of $\dot{V}(E)$ and therefore, $\dot{V}(E) < 0$. In the case when $N_O^i = 0$, the trajectories satisfy $\|E^{ij}\| < r^{ij}$, for all $i = 1, \ldots, N$, and $j \in \mathcal{N}_i$. Therefore, we can take $\max_{i,j} r^{ij}$ as the ultimate bound.

So far we have shown the conditions to achieve uniform ultimate boundedness for each E^{ij}. This result shows that if the difference in position and velocity of between an individual and his or her neighbors is sufficiently large, then the trajectories of position and velocity will behave such that this difference decreases until it reaches a boundary. To complete the proof, we have to show that the error in position and velocity between every two individuals in the group is bounded when $\|E^{ij}\|$, for all $i, j \in \{1, \ldots, N\}$, is bounded. Assume that the uniform ultimate boundedness has been achieved in the trajectories of the error system (19), and $\|E^{ij}\| < r^i$ for all $i \in \{1, \ldots, N\}$ and $j \in \mathcal{N}_i$. Let $i \to j$ denote that individual i is a neighbor of j in the communication network, that is, $i \in \mathcal{N}_j$. Let $l_1 \to l_2 \to \cdots \to l_M$ denote the directed path starting from l_1 and ending in l_M, where $l_i \in \{1, \ldots, N\}$. We know that for $l_1 \to l_2$ and $l_2 \to l_3$, it is true that $\|E^{l_2 l_1}\| < r^{l_2 l_1}$ and $\|E^{l_3 l_2}\| < r^{l_3 l_2}$. Since the error term $\|E^{ij}\|$ is a weighted Euclidean distance in position and velocity between individuals i and j, we have that $\|E^{l_3 l_1}\| \leq \|E^{l_2 l_1}\| + \|E^{l_3 l_2}\| < r^{l_2 l_1} + r^{l_3 l_2}$. Applying sequentially this relation to the directed path $l_1 \to l_2 \to \cdots \to l_M$, we obtain

$$
\|E^{l_M l_1}\| < \sum_{j=1}^{M-1} r^{l_{j+1} l_j} = r^{l_M l_1}.
\tag{38}
$$

Therefore, from the assumption that there is a directed path between every two nodes, if the trajectories of the error system (19) achieve uniform ultimate boundedness, then there exists a bound for $\|E^{ij}\|$ for every $i, j \in \{1, \ldots, N\}$. ∎

Remark 1: This result shows that, when the assumptions on the parameters of the model and the communication topology are satisfied, if the $\|E_{ij}\|$ are large enough, then the trajectories of the error system will achieve uniform ultimate boundedness. This means that if the individuals in the group are sufficiently separated in position and velocity from the other members, they will move closer to them in a way that the uniform ultimate bound for position and velocity is satisfied.

Remark 2: This analysis provides information about conditions that are sufficient to have cohesiveness in the group, but it does not state any condition on achieving local optimality of the performance function.

Remark 3: The assumptions on the boundedness of the difference in performance and the gradient of the performance function in (20) and (21) are reasonable assumptions that can be satisfied by realistic performance functions such as a mixture of Gaussian functions and a plane, and hence they do not represent a restrictive condition for our analysis.

Remark 4: The assumption that the communication network is represented by a strongly connected graph indicates that every individual in the group influences any other group member either by a direct connection, or indirectly by a "chain effect." The latter means that, since there is a direct path in communication between every two members of the group, every individual can indirectly affect the dynamics of every other group member as (38) indicates. If this assumption is not satisfied, from the proof of Theorem 1, cohesiveness can only be guaranteed between an individual and his or her direct neighbors.

Remark 5: Constant c_1^{ij} in (32) gives us information about the strength in attraction from individual i to j with respect to the influence of the other components that drive the dynamics of i. On the other hand, c_2^{ij} and c_3^{ij} corresponds to the strength of the other components that influence the individual's behavior such as the task to optimize, and repulsions and attractions to other individuals. Then, (22) and (23) indicate that if the influence of the attraction from i to j represented in c_1^{ij} is stronger than the influence of the rest of the components of the behavior of individual i represented in c_3^{ij}, then it is guaranteed that there is a bound of the error in position and velocity between i and j that will be satisfied at some finite time.

Remark 6: Note that from (22) and (23), the conditions for ultimate uniform boundedness do not depend on the parameters of the component of the force u^i in (3) that is associated with repulsion between individuals. However, from (33), we see that the parameters of the repulsion term do affect the size of the ultimate bound through the constant c_2^{ij}.

Remark 7: Note that when the repulsion and the optimization of the performance function do not have any influence in the computation of the force u^i in (3) (i.e., $r(t) = p(t) = 0$), from (33) we have that $c_2^{ij} = 0$, and $\Pi_O^i = \mathcal{N}_i$. Then, if the condition (36) is satisfied for all $t \geq 0$, the uniform ultimate bound will be as tight as possible in this setting. If we additionally assume that the attraction weights w^{ij} and the

performance optimization parameters η^i are constant, this particular case of our model is known as a "consensus algorithm" for double-integrator dynamics [25, Ch. 4].

IV. DYNAMICS OF THE GROUP IN COMPLEX TASK ENVIRONMENTS

We explore the dynamics of the group when its members have to solve a given task, which is defined by f. Recall that N denotes the number of members in the group. We choose $x^i \in \mathbb{R}^2$ for all $i = 1, \ldots, N$, and $f : \mathbb{R}^2 \to \mathbb{R}$ to be a continuously differentiable function. We consider two different complex task environments: first, we choose a function that has three local minima, three local maxima, one global minimum x^* such that $f(x^*) = 0$, and flat regions. The equation of this function is

$$f(x_1, x_2) = 3(1 - x_1)^2 \exp\left[-\left(x_1^2\right) - (x_2 + 1)^2\right]$$
$$- 10\left(\frac{x_1}{5} - x_1^3 - x_2^5\right) \exp\left(-x_1^2 - x_2^2\right)$$
$$- \frac{1}{3} \exp\left[-(x_1 + 1)^2 - x_2^2\right] + 6.5511.$$

Fig. 1 shows a contour plot of this function. This function allows us to study the behavior of the group when the task-solving process can lead to different solutions.

In the second scenario, we choose a function defined by a plane. This function allows us to study the dynamics of the group in terms of performance and cohesion when the task-solving process is continual, and does not have a fixed solution point. To quantify the group cohesion and performance at a given time t, we define three measurements: group cohesion in position, defined as

$$\gamma(t) = -\frac{1}{N(N-1)/2} \sum_{i,j \in \mathcal{V}} \left\| x^i(t) - x^j(t) \right\|^2 \qquad (39)$$

is the negative sum of the pairwise distances between the individuals at time t. This function allows us to quantify how close the group members are to each other at a given time. We have $\gamma(t) = 0$ when all the individuals are at the same position, and negative values of $\gamma(t)$ indicate separation between the group members. Similarly, we have the group cohesion in velocity, defined as

$$\gamma_v(t) = -\frac{1}{N(N-1)/2} \sum_{i,j \in \mathcal{V}} \left\| v^i(t) - v^j(t) \right\|^2. \qquad (40)$$

In addition to cohesion measurements, we define Group performance as

$$J(t) = -\frac{1}{N} \sum_{i=1}^{N} f\left(x^i(t)\right) \qquad (41)$$

which is the negative sum of the individual performance of each group member. This function allows us to measure how the group is performing in solving the task at time t. Below, we present the results of the simulations of the dynamics of the group under different scenarios in the topology of the communication network, parameters of the model, and flow of information.
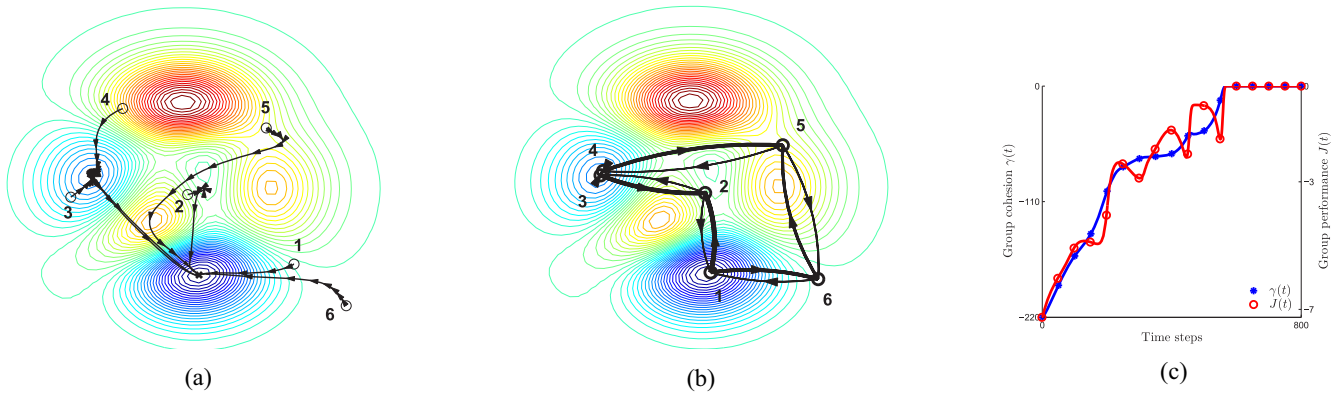
Fig. 1. (a) Contour of the cost function $f(x)$ and trajectory of the members of the group (black solid lines), where symbol "o" indicates the initial position, and the arrows represent the direction of their trajectory. (b) Contour of the performance function and communication network in the group, where the arrows indicate the flow of the information, the thickness of the line indicates the strength in attraction between members, and the symbol "o" marks the location of the individual at time step 150. (c) Cohesion $\gamma(t)$ and performance $J(t)$ of the group.

A. Trajectories and Attraction Patterns in the Group

To illustrate the group dynamics that can be generated using the proposed model, we first study the performance and cohesion of the group and the trajectories of each individual given a set of initial conditions and parameters of the model and the performance function f that has multiple solutions. In this case, the group is composed of $N = 6$ individuals, whose initial position is randomly selected and initial velocities are set to 0. Also, $w_{ij}(0) = 1/|\mathcal{N}_i|$ for every $i \in \mathcal{V}$ and $j \in \mathcal{N}_i$. The parameters of the model are chosen such that at $t = 0$ the contribution of the term associated with the gradient of the function $\nabla f(x^i(t))$ in (3) is large compared to the one associated with the attractions $a^i(t)$, and the short-range repulsion in position between individuals is very small. To facilitate the analysis of the attraction patterns of the group, in this simulation there is no attraction in velocity, that is, $b = 0$. The communication network between the group members follows a symmetric ring topology (each node has two neighbors). This means that each group member communicates with his or her contiguous group members via a bidirectional flow of information. The discretization of the differential equations is done using Euler's approximation method with sampling time $T = 0.1$. Fig. 1 shows the behavior of the individuals at different time steps. From the trajectory of the agents in Fig. 1(a), we can observe that initially the individuals tend to go to their closest local minimum or saddle point. This is due to the fact that initially the force that drives each individual is more oriented toward solving the task than being attracted to the rest of the group. However, individuals start increasing their attraction to those that are connected to them and have a better relative performance as Fig. 1(b) illustrates. There is a point where the attraction weights become large enough that the force driving the individuals points toward those individuals with better relative performance, even if it implies moving in a direction that locally does not optimize its performance. Note that, since the agents are not fully interconnected, some individuals sequentially jump to minima until eventually they reach the global one. This behavior is evident in Fig. 1(c), where the group performance decreases at some points where group cohesion increases.

A further interpretation of the mathematical model in (2)–(8) allows us to explain the attraction patterns in the dynamics observed in Section IV. Using simple algebraic operations, we can rewrite the component associated with the attraction in position and velocity in (5) as

$$a^i(t) = -\bar{w}^i(t)\big(x^i(t) - \bar{x}^i(t)\big) - b\bar{w}^i(t)\big(v^i(t) - \bar{v}^i(t)\big) \quad (42)$$

where $\bar{w}^i(t) = \sum_{j \in \mathcal{N}_i} w^{ij}(t)$ is the sum of the attraction in position strengths. We have that

$$\bar{x}^i(t) = \bar{w}^i(t)^{-1} \sum_{j \in \mathcal{N}_i} w^{ij}(t) x^j(t)$$

corresponds to the weighted average of the position of the individuals in $\mathcal{N}_i$. Here, $\bar{x}^i(t)$ is located closer to those individuals in $\mathcal{N}_i$ with higher attraction strength. In a similar way, we can compute $\bar{v}^i(t)$. During the process of solving the task, from (7), we have that an individual tends to be more attracted to the ones that are performing better than him or her, that is, have a higher contribution in the computation of the weight average $\bar{w}^i(t)$. As some of the w^{ij} increase, term $\bar{w}^i(t)$ in (42) becomes larger and the influence of the attraction component in force $u^i(t)$ becomes significantly larger than the component associated with performance optimization. In Fig. 1, we can observe that group members that initially move to local minima or saddle points later move toward those individuals that have better performance. For example, individual 2 moves to a saddle point, but later it gets attracted to 1, who is performing better. Also, individual 3 reaches a local minimum, but it later climbs up the valley because it gets attracted to individual 2 who is performing better (because 2 is being attracted to 1). These dynamics allow the group to eventually reach the global minimum and remain cohesive.

B. Topology of the Communication Network

In the next set of simulations, we explore the behavior of the cohesion and performance of the group to solve the given task under different communication topologies. We estimate group cohesion $\gamma(t)$ and group performance $J(t)$ in (39) and (41) using the Monte Carlo simulation method by repeating the simulations 1000 times with different initial
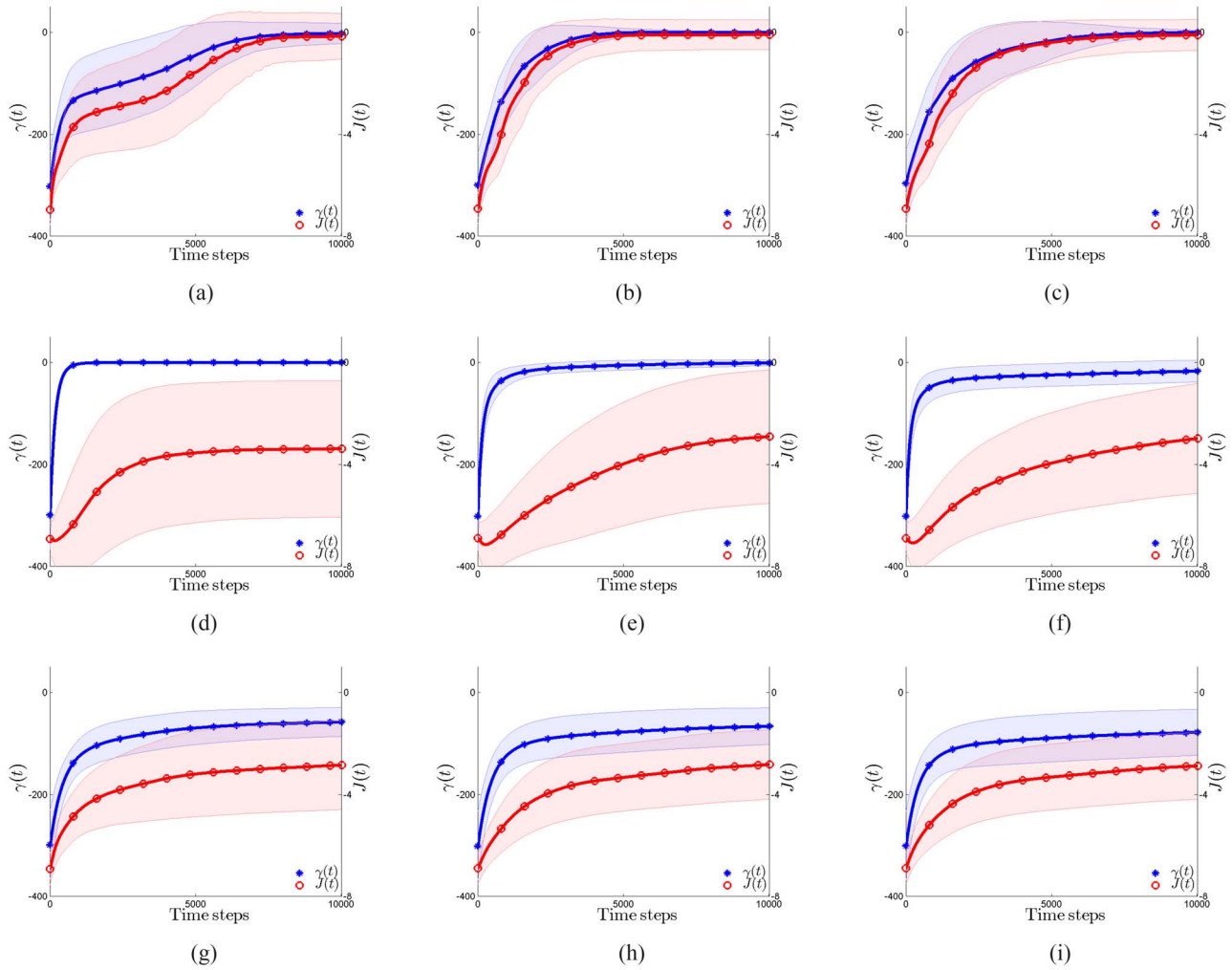
Fig. 2. Mean (solid line) and standard deviation (shaded region) of group cohesion $\gamma(t)$ and group performance $J(t)$ estimated using Monte Carlo simulations for a group with ten members under (a), (d), (g) wheel, (b), (e), (h) ring, and (c), (f), (i) line communication networks. Simulations are performed in three different scenarios: (a)–(c) dynamics on the attraction and performance weights, (d)–(f) constant and equal attraction weights, where the attraction term has a predominance in the behavior of the individuals, and (g)–(i) constant and equal attraction weights, where both the attraction term and gradient of the cost function affect the behavior of the individuals.

conditions each time. This number of repetitions allows us to obtain a good estimate of the means and standard deviations of $\gamma(t)$ and $J(t)$. We create a group with $N = 10$ members, whose initial conditions in position are randomly selected, and initial velocities are set to zero. The performance function is the one that has several local minima. The discretization of the differential equations is done using Euler's approximation method with sampling time $T = 0.01$.

We simulate the model under different topologies of the network that define how the members of the group communicate between each other. First, we compute group cohesion and performance under three topologies: a wheel, in which most of the members of the group communicate with only one individual. A ring, in which every individual communicates with only two other group members. And a line, in which is similar to the ring topology but two of the group members communicate with only one individual. For each topology, the parameters of the model are chosen under three different scenarios: 1) as in the simulation in Fig. 1, where the performance optimization component of force u^i is initially

stronger than the attraction ones; 2) dynamics for the attraction weights and performance optimization strength (i.e., $\alpha_w = 0$ and $\alpha_\eta = 0$), in which the attraction strength is significantly larger than that of performance optimization; and 3) again no dynamics for the attraction weights and performance optimization strength (i.e., $\alpha_w = 0$ and $\alpha_\eta = 0$), but in this case the attraction and performance optimization strengths have a similar influence on the force u^i.

Fig. 2(a)–(i) show the results for each case. In the first scenario, where the dynamics of the attraction weights and strength in performance optimization is given by (7) and (8), we can observe that the average group cohesion $\gamma(t)$ and average group performance $J(t)$ reach a value close to zero, which means that all the members of the group reach almost the same position, and they achieve the global optimum. However, depending on the topology, there are significant differences in the trajectories that the group follows. It can be observed that the group in a wheel-type communication network [Fig. 2(a)], compared to the other two network topologies, takes longer to reach a state in which the group can be considered as

cohesive and has larger variability in the trajectories of $\gamma(t)$ and $J(t)$ for different initial conditions. The communication network that with better performance is the one with a ring-type topology [Fig. 2(b)]. The time the group takes to achieve a steady state and the variability for different initial conditions in performance and cohesion is considerably shorter than the other two topologies. These results are consistent with observations of human groups solving complex tasks [3], [13]. It has been reported that groups tend to perform better in decentralized communication networks (ring) than centralized ones (wheel).

In the second scenario, the parameters in attraction and performance optimization have no dynamics, and the contribution of the attraction term to the force that drives the members of the group is higher than the contribution of the performance optimization. In this case, the group reaches an agreement. However, the position that the group agrees at has a large variability, and on average, it does not correspond to the global minimum. In the third scenario, the attraction and performance optimization parameters have no dynamics, but in this case they have equal contribution to the force u^i. In this case, on average, neither $\gamma(t)$ nor $J(t)$ are maximized.

C. Density of the Communication Network

To observe the effect of the density of the topology on the cohesion and performance of the group, we used the Monte Carlo simulation method with 1000 repetitions to estimate group cohesion and group performance in a group with $N = 50$ members. The parameters are chosen as in the simulations in Section IV-A. The selected performance function is the one that has several local minima. The density of a network topology is defined as the number of connections divided by the total possible number of connections between the members of the group. A density of 1 corresponds to a fully connected network. Fig. 3 shows the results of the simulation for a network with a ring topology, where each node has 25 neighbors, and a network that is fully connected. This corresponds to networks that have densities 0.4898 and 1, respectively. In Fig. 3, we can observe that as the number of neighbors increases, the time it takes to the members of the group to be considered cohesive increases, and the performance of the whole group decreases. This behavior can be noted from (5) and (6). Here, the attraction, repulsion, and performance optimization terms are scaled by $|\mathcal{N}_i|^{-1}$. When the number of neighbors increases, then the force that directs the motion of the individuals is mostly influenced by the term $-\zeta^i v^i$, $i = 1, \ldots, N$, which makes the velocities of the individuals decrease. This behavior has been observed in human groups [3], [10]. It has been shown that the size of the group significantly affects both cohesion between members and the performance during the task-solving process. In the model, term $|\mathcal{N}_i|^{-1}$ in the social force components accounts for this effect. When the number of neighbors increases, then the social influence on the dynamics of the individual decreases. As the cohesive behavior of the group decreases, the overall performance of the group also is affected.
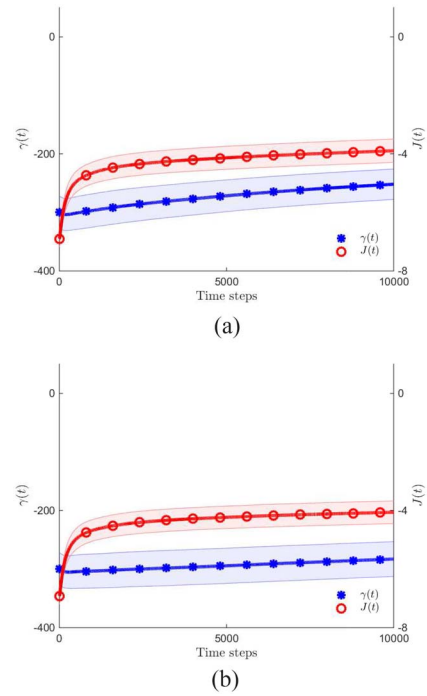

Fig. 3. Mean (solid line) and standard deviation (shaded region) of group cohesion $\gamma(t)$ and group performance $J(t)$ estimated using Monte Carlo simulations for communication networks in groups with 50 members. (a) With a ring-type topology where each node has 25 neighbors. (b) Fully connected topology.

D. Group Dynamics in Task Environment Represented by Plane

A task environment f given by a plane with respect to the position of the individuals in the group allows the group to have a continual optimization process of its performance during the selected time interval of analysis. In this case, the component of the force u^i associated with the performance optimization is constant and different from zero. In this set of simulations we measure the cohesion of the group in position and velocity and its performance for the wheel, ring, and line communication network topologies used in the previous set of simulations (see Fig. 2). The communication network has a ring topology, and the parameters are chosen such that there is an interaction between the attraction and performance components of the force that drive the motion of the group as in Section IV-A. However, in this case the attraction term depends not only on position but also in velocity. To study the behavior of cohesion and performance in the group, we used the Monte Carlo simulation method with 1000 repetitions, and estimated the mean and standard deviation of the group cohesion in position and velocity, and group performance, measured y $\gamma(t)$, $\gamma_v(t)$, and $J(t)$, respectively. Fig. 4 shows these measurements for different communication network topologies. Note that the group in a wheel topology reaches significantly faster cohesiveness in position than the ring and line topologies. However, there is a larger variability in the initial behavior of the velocity vector and in the performance of the group. The groups working in ring and line topologies take longer to reach a state considered as cohesive, but their performance has less
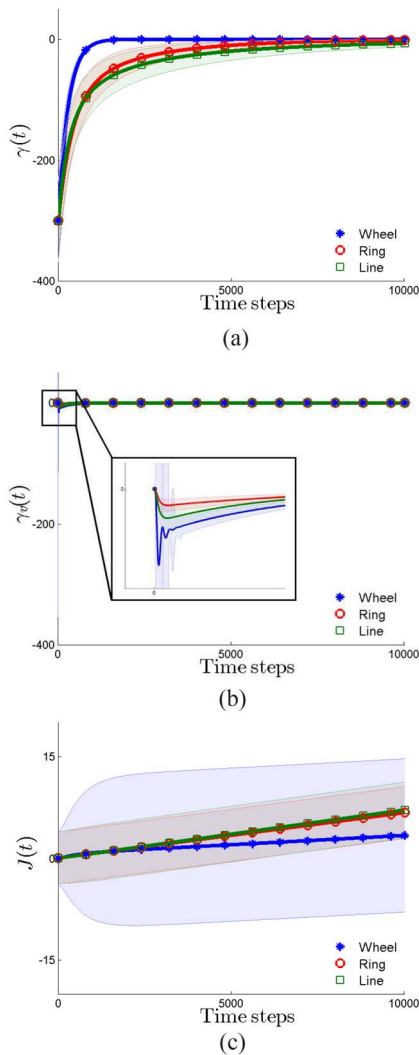
Fig. 4.   Mean and standard deviation of group cohesion in (a) position and (b) velocity, and (c) performance of the group for different communication topologies and when the performance function is characterized by a plane. The solid line and the shaded region correspond to the mean and standard deviation estimated using Monte Carlo simulations.

variability and increases faster than the one obtained by the groups working in a wheel topology.

V. Conclusion

We developed a model of a group of individuals that interact according to a communication network, and whose dynamics are driven by a component that seeks to optimize a task and the influence of the interactions of the group members. The key aspect in our model, which is the main difference with other models of group dynamics and consensus, is that the strength of the social influence and the commitment to solve the task are not static but dynamic, and depend on the relation between cohesion and performance of the group. Simulation results show that the relation between cohesion and performance, described in (7) and (8), allows the model to characterize dynamics that are qualitatively consistent with the results observed in human groups. It is shown that, in average, decentralized communication network topologies outperform

the centralized ones when solving a complex task, and a larger number of connections between individuals decreases cohesion and task performance. Also, a theoretical analysis of the model shows that, under the appropriate conditions on the parameters and topology of the network, the group reaches a point where it is considered as cohesive.

This model represents a tool for the analysis and design of communication networks of task-solving groups. It enables the social scientist to understand human groups as a dynamical system, to explore the group behaviors under different conditions in the parameters and network topology, and to design new methodologies for the development of experiments in real-human groups whose aim is to solve complex tasks.

References

[1] G. C. Homans, *The Human Group*. Routledge, London, U.K., 1951.

[2] A. Pentland, T. Choudhury, N. Eagle, and P. Singh, "Human dynamics: Computation for organizations," *Pattern Recognit. Lett.*, vol. 26, no. 4, pp. 503–511, 2005.

[3] D. R. Forsyth, *Group Dynamics*, 5th ed. Belmont, CA, USA: Cengage Learn., 2009.

[4] N. Triplett, "The dynamogenic factors in pacemaking and competition," *Amer. J. Psychol.*, vol. 9, no. 4, pp. 507–533, Jul. 1898.

[5] K. Lewin, *Field Theory in Social Science*. New York, NY, USA: Harpers, 1951.

[6] L. Festinger, "Informal social communication," *Psychol. Rev.*, vol. 57, no. 5, pp. 271–282, 1950.

[7] J. A. Davis, "Structural balance, mechanical solidarity, and interpersonal relations," *Amer. J. Sociol.*, vol. 68, no. 4, pp. 444–462, 1963.

[8] C. N. Alexander, "Consensus and mutual attraction in natural cliques a study of adolescent drinkers," *Amer. J. Sociol.*, vol. 69, no. 4, pp. 395–403, 1964.

[9] D. Levi, *Group Dynamics for Teams*. Thousand Oaks, CA, USA: Sage, 2001.

[10] B. Mullen and C. Copper, "The relation between group cohesiveness and performance: An integration," *Psychol. Bull.*, vol. 115, no. 2, pp. 210–227, 1994.

[11] D. J. Beal, R. R. Cohen, M. J. Burke, and C. L. McLendon, "Cohesion and performance in groups: A meta-analytic clarification of construct relations," *J. Appl. Psychol.*, vol. 88, no. 6, pp. 989–1004, 2003.

[12] H. J. Leavitt, "Some effects of certain communication patterns on group performance," *J. Abnormal Soc. Psychol.*, vol. 46, no. 1, pp. 38–50, 1951.

[13] M. E. Shaw, "Communication networks," in *Advances in Experimental Social Psychology*, vol. 1. New York, NY, USA: Academic Press, 1964, pp. 111–147.

[14] N. Katz, D. Lazer, H. Arrow, and N. Contractor, "Network theory and small groups," *Small Group Res.*, vol. 35, no. 3, pp. 307–332, 2004.

[15] U. A. Segal, "The cyclical nature of decision making: An exploratory empirical investigation," *Small Group Behav.*, vol. 13, no. 3, pp. 333–48, 1982.

[16] T. M. Brown and C. E. Miller, "Communication networks in task-performing groups: Effects of task complexity, time pressure, and interpersonal dominance," *Small Group Res.*, vol. 31, no. 2, pp. 131–157, 2000.

[17] D. Helbing, "A mathematical model for the behavior of individuals in a social field," *J. Math. Sociol.*, vol. 19, no. 3, pp. 189–219, 1994.

[18] A. Pentland and A. Liu, "Modeling and prediction of human behavior," *Neural Comput.*, vol. 11, no. 1, pp. 229–242, 1999.

[19] M. Moussaïd, N. Perozo, S. Garnier, D. Helbing, and G. Theraulaz, "The walking behaviour of pedestrian social groups and its impact on crowd dynamics," *PLoS One*, vol. 5, no. 4, 2010, Art. ID e10047.

[20] V. Gazi and K. M. Passino, "Stability analysis of social foraging swarms," *IEEE Trans. Syst., Man, Cybern. B, Cybern.*, vol. 34, no. 1, pp. 539–557, Feb. 2004.

[21] R. Olfati-Saber, J. A. Fax, and R. M. Murray, "Consensus and cooperation in networked multi-agent systems," *Proc. IEEE*, vol. 95, no. 1, pp. 215–233, Jan. 2007.

[22] W. Li, "Stability analysis of swarms with general topology," *IEEE Trans. Syst., Man, Cybern. B, Cybern.*, vol. 38, no. 4, pp. 1084–1097, Aug. 2008.

[23] W. Yu, G. Chen, M. Cao, and J. Kurths, "Second-order consensus for multiagent systems with directed topologies and nonlinear dynamics," *IEEE Trans. Syst., Man, Cybern. B, Cybern.*, vol. 40, no. 3, pp. 881–891, Jun. 2010.

[24] X. Wang, S. Li, and P. Shi, "Distributed finite-time containment control for double-integrator multiagent systems," *IEEE Trans. Cybern.*, vol. 44, no. 9, pp. 1518–1528, Sep. 2014.

[25] W. Ren and R. Beard, *Distributed Consensus in Multi-Vehicle Cooperative Control: Theory and Applications*. London, U.K.: Springer, 2007.

[26] P. A. Forero, A. Cano, and G. Giannakis, "Consensus-based distributed support vector machines," *J. Mach. Learn. Res.*, vol. 11, pp. 1663–1707, May 2010.

[27] J. A. Giraldo, E. Mojica-Nava, and N. Quijano, "Synchronization of isolated microgrids with a communication infrastructure using energy storage systems," *Int. J. Elect. Power Energy Syst.*, vol. 63, pp. 71–82, Dec. 2014.

[28] D. Helbing, *Quantitative Sociodynamics*. Berlin, Germany: Springer, 2010.

[29] Y. Liu and K. M. Passino, "Stable social foraging swarms in a noisy environment," *IEEE Trans. Autom. Control*, vol. 49, no. 1, pp. 30–44, Jan. 2004.

[30] R. M. Roe, J. R. Busemeyer, and J. T. Townsend, "Multialternative decision field theory: A dynamic connectionst model of decision making," *Psychol. Rev.*, vol. 108, no. 2, pp. 370–392, 2001.

[31] M. Usher and J. L. McClelland, "Loss aversion and inhibition in dynamical models of multialternative choice." *Psychol. Rev.*, vol. 111, no. 3, pp. 757–769, 2004.

[32] H. K. Khalil, *Nonlinear Systems*, 3rd ed. Upper Saddle River, NJ, USA: Prentice Hall, 2002.

[33] M. Zedek, "Continuity and location of zeros of linear combinations of polynomials," *Proc. Amer. Math. Soc.*, vol. 16, no. 1, pp. 78–84, 1965.

[34] G. H. Golub and C. F. V. Loan, *Matrix Computations*. Baltimore, MD, USA: Johns Hopkins Univ. Press, 2013.

Luis Felipe Giraldo is currently pursuing the Ph.D. degree in electrical and computer engineering from the Ohio State University, Columbus, OH, USA.

His current research interests include modeling and analysis of linear and nonlinear dynamical systems, pattern recognition, and signal processing.

Kevin M. Passino (S'79–M'90–SM'96–F'04) received the PhD degree in electrical engineering from the University of Notre Dame, Notre Dame, IN, USA, in 1989.

He is a Professor of Electrical and Computer Engineering and the Director of the Humanitarian Engineering Center with the Ohio State University, Columbus, OH, USA. He has published a book entitled *Humanitarian Engineering: Creating Technologies that Help People, Edition 2* (Columbus, OH, USA: Bede, 2015).